A Hybrid Energy Storage System for flexibility provision: Modeling and Control design

Jemma J. Makrygiorgou [1,2,*], Despoina I. Makrygiorgou[1,2], Serafeim Panidis[1],
Christos Dikaiakos [1], Jun Rong [1], Antonio T. Alexandridis [2],

1 Independent Power Transmission Operator, Dyrrachiou 89 & Kifissou, 10443, Athens
2 Department of Electrical and Computer Engineering, University of Patras, Rion 26504, Greece

Abstract—The increasing power demand and the high penetration of renewable energy sources (RES), among with grid security, and stability make the need of flexibility a major challenge. Different methods have been identified to meet this need, of which the integration of the power sources with storage provides one of the most prominent ones. Moreover, hybridization of storage systems is a new trend with guaranteed benefits. In this paper, the potential of a proposed hybrid energy storage system (HESS) and its control scheme regarding the RES integration and grid stability, is under investigation. The HESS consisting of supercapacitor (SC) cells and a battery array that can interchange flexibility between RES units and the utility grid. Power electronic devices act as interfaces that aiming to meet the flexibility needs in real-time and guaranteeing the balancing between RES production, load, and grid fluctuations. Control structure based on hierarchical and cascaded control are applied. The obtained closed-loop HESS is evaluated under varying conditions and the results fully verify that the flexibility is activated in real-time transients, once the high-performance control schemes are applied such that the frequency and dc and ac voltage are regulated quickly and smoothly.

Index Terms—hybrid energy storage system, flexibility, cascaded control, power converters, battery, supercapacitor

I. INTRODUCTION

Within a proper power system performance, electricity supply needs to be always balanced with electricity demand and network losses. However, the inherent intermittent and stochastic nature of Renewable Energy Sources (RES) is constantly modifying the time dynamics of net-demand; it poses uncertainty in meeting the energy demand and maintaining power system stability-voltage and frequency regulation [1], [2]. Hence, a need for flexibility in the power system network arises. Flexibility indicates the capacity of a power system network to reliably sustain supply during transient and large imbalances caused by both anticipated and unanticipated variability [3], [4]. Flexibility services are provided by actors within the power grid that facilitate and support the continuous power flow, so that the demand for electrical energy is met in real-time. These operations generally include active power control or frequency control and reactive power control or voltage control, on various timescales [3], [4]. Traditionally, such services have been provided by large production units, such as generators. Nowadays, increasing RES mix in power grids,

with smart grid technologies and advanced power electronics converters bring smaller distributed generation, consumption, and storage units to meet the flexibility demands [4], [5].

In this framework, Energy Storage Systems (ESS) are to play a key role in distribution and transmission networks in the following years [4], [5]. These devices increase both the production systems' performance and flexibility of power systems. There are numerous requirements for an energy storage to be successfully applied in a flexibility provision application such as high specific energy and energy density, high specific power and power density, long cycle lifetime, efficiency, low cost, maintenance, recycleability, etc. In most cases, all those requirements cannot be satisfied by a single energy source. Therefore, the only viable solution is the hybridization of the ESS [6], [7]. Overall, the utilization of the supercapacitors (SCs) in combination with the batteries, can be characterized as beneficial and yield some benefits regarding the grid's stability and efficiency [6], [7]. The major identified advantages and the drawbacks related to the application of Hybrid Energy Storage Systems (HESSs) are summarized in the Table I.

TABLE I: Advantages & Disadvantages of HESS

Advantages	Drawbacks
Capability of the voltage and frequency regulation	Requirement of Power Electronics and control modes
Wide operating range	Low Energy Density
High Power Density	High Installation Cost
Long Lifespan	Risk of over-voltage of the cells
High Efficiency	

Several studies investigate HESS, specifically storage systems that includes both batteries and SCs. Manandhar et al. [8] propose an energy system management for a HESS, including a battery and SC, under several operating conditions, which results in a faster dc-link voltage mitigation. Barath et al. [9] present the application of the SC for the improvement of the power quality/reactive power regulation on the transmission grid, while Nguyen et al. in [10] and Arkhangeski et al. in [11] introduce HESS, as an effective solution for the frequency regulation. Rocabert et al. [12] propose a droop control, for the optimization of the power flow between the battery and the SC subsystems, while Malkawi et al. [13] described the main advantage of using a SC along with the batteries.

In all previous cases, the use of HESS for flexibility provision to the grid, concentrates only on the system technical de-

scription and on management techniques. In addition, system modeling concerns partially dynamic behaviour and never by taking into account the complete nonlinear dynamic model of the system. To this end, in the present study a HESS consisting of SC units and a battery array that can interchange flexibility between the different RES and the utility grid is proposed and implemented. Power electronic devices are considered that act as interfaces while offering a critical opportunity for controlling the power transferred through them via realizing control commands at the power grid level [14]. The proposed and developed model includes detailed mathematical representations of all critical subsystems; i.e the HESS, the dc-link, the LCL filter that interfaces the storage system to the grid, accompanied by the essential power electronic converters. The overall system can tackle the frequency and voltage transients guaranteeing the power system balancing in real time.

Keeping in mind the extracted dynamic model, control structure based on hierarchical control levels are applied for frequency and voltage control applying also a Phase Locked Loop (PLL) synchronism circuit [15]. To the best of the authors knowledge, the control design for such complex systems and after considering the entire nonlinear system representation has not yet been reported. In the present study, the familiar industrial engineers cascaded Proportional Integral (PI) controllers are proposed [16], [17] and implemented aiming at the optimal system operation despite grid disturbances via i) operating the HESS under constant voltage, ii) achieving zero reactive power injection to the grid, and iii) operating the power converters under sinusoidal pulse width modulation (SPWM). The overall system is evaluated through extended simulations, under varying RES, load and grid conditions, offering flexibility services locally to the grid. The results verify that the flexibility will be activated real time during transients since the high-performance control schemes are applied on each power interface such that the frequency and dc and ac voltage are quickly regulated.

The rest of the paper is organized as follows. In section II, the entire HESS to grid system is represented by an accurate dynamic model. In section III, a suitable control scheme is proposed and designed by keeping in mind the complete nonlinear system representation. In section IV, the entire system is examined via extended simulations under various scenarios and flexibility needs and finally, in section V, the extracted results are discussed and some conclusions are drawn.

II. SYSTEM MODEL

Towards analysing and controlling the entire system that coordinates the power flow between the grid and the HESS, its accurate dynamic representation deemed necessary. A general architecture is provided in **Fig. 1**. It is comprised of a HESS that is connected to the dc-link via a dc/dc bidirectional boost converter, which enables the power flow between the grid and the HESS. Furthermore, the dc-link exchanges energy with the grid among an ac/dc voltage source converter that is connected to the ac grid through an LCL filter. The dynamic behaviours of the aforementioned subsystem are described

by their accurate mathematical representation, in the $d-q$ synchronously rotating reference frame [14], that achieves their proper simulation and analysis. The basic advantage of this representation is that the state variables of the system are transformed from sinusoidal to constant quantities at steady state, which facilitates the effective design of simple PI controllers.

A. Battery

The first component of the HESS comprises of a Li-on battery pack and is described by a second order Thevenin model [6], [18], eq. (1)-(4). The filter involves a voltage drop V_o, an internal resistance R_{ser} and two resistance capacitance (RC) pair that represent the transient phenomenon, **Fig. 1**.

$$V_{bat} = V_o - V_s - V_l - R_{ser} \cdot I_{bat} \qquad (1)$$

$$\dot{V_l} = -\frac{V_l}{R_l \cdot C_l} + \frac{I_{bat}}{C_l} \qquad (2)$$

$$\dot{V_s} = -\frac{V_s}{R_s \cdot C_s} + \frac{I_{bat}}{C_s} \qquad (3)$$

$$C_{cap} \cdot SoC_{bat} = SoC_{bat}(0) - \int I_{bat} \cdot d\tau \qquad (4)$$

where V_{bat}, I_{bat} stand for the battery voltage and current, respectively, V_s and V_l relate to the voltage drops on the RC pairs. In addition, SoC_{bat} represents the battery's state of charge and $SoC_{bat}(0)$ relates to its initial value. All other battery parameters are given in Table II.

B. Supercapacitor

The SC dynamics are adequately represented by the simplified equivalent model, [19], eq. (5)-(8). It includes a series resistance R_{sc}, a series capacitor C_{sc} that provides the SC capacitance, and RC parallel branch R_{c1}, C_{c1}, **Fig. 1**.

$$V_{sc} = V_{co} - V_{c1} - R_{sc} \cdot I_{sc} \qquad (5)$$

$$C_{sc} \cdot \dot{V}_{co} = -\gamma \cdot V_{co} + I_{sc} \qquad (6)$$

$$C_{c1} \cdot \dot{V}_{c1} = -\frac{1}{R_{c1}} \cdot V_{c1} + I_{sc} \qquad (7)$$

$$C_{sc} \cdot SoC_{sc} = SoC_{sc}(0) - \int I_{sc} \cdot d\tau \qquad (8)$$

where V_{sc} and I_{sc} are the output dc voltage and current of one SC cell, respectively, V_{c1} stands for the voltage across the R_{c1}, C_{c1} parallel branch, and V_{co} represents the voltage drop on the R_{sc}, C_{sc} series branch. In addition, SoC_{sc} represents the battery's state of charge and $SoC_{sc}(0)$ relates to its initial value. The parameters' values are provided in the Table II.

C. LCL Filter

Different types of filters can be used to interface the voltage source converter to the grid. In the present study, a LCL filter is adopted able to mitigate the switching harmonic currents. Its mathematical dynamic representation in the $d-q$
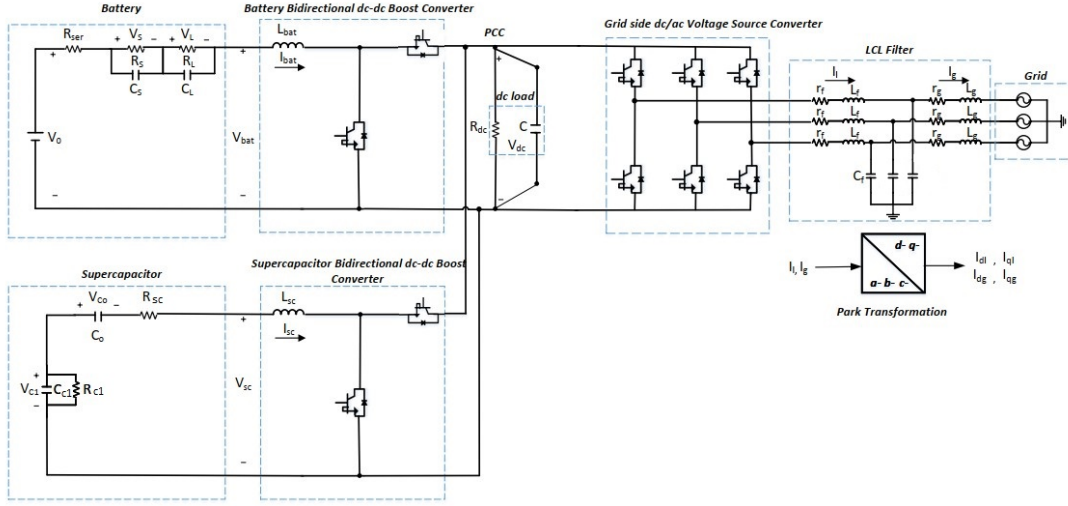
Fig. 1: The entire HESS to grid system architecture.

synchronously rotating reference frame, is given in eq. (9) - (14).

$$L_f \cdot \dot{I}_{dl} = -r_f \cdot I_{dl} + m_d \cdot V_{dc} - V_d + L_f \cdot \omega_{pll} \cdot I_{ql} \quad (9)$$

$$L_f \cdot \dot{I}_{ql} = -r_f \cdot I_{ql} + m_q \cdot V_{dc} - V_q - L_f \cdot \omega_{pll} \cdot I_{dl} \quad (10)$$

$$C_f \cdot \dot{V}_d = I_{dl} - I_{dg} + C_f \cdot \omega_{pll} \cdot V_q - \frac{V_d}{R_{ac}} + \\ + I_{res,ac,d} - I_{load,ac,d} + I_{gen,ac,d} \quad (11)$$

$$C_f \cdot \dot{V}_q = I_{ql} - I_{qg} - C_f \cdot \omega_{pll} \cdot V_d - \frac{V_q}{R_{ac}} + \\ + I_{res,ac,q} - I_{load,ac,q} + I_{gen,ac,q} \quad (12)$$

$$L_g \cdot \dot{I}_{dg} = -r_g \cdot I_{dg} + V_d - V_{d,grid} + L_g \cdot \omega_{grid} \cdot I_{qg} \quad (13)$$

$$L_g \cdot \dot{I}_{qg} = -r_g \cdot I_{qg} + V_q - V_{q,grid} - L_g \cdot \omega_{grid} \cdot I_{dg} \quad (14)$$

where I_{dl}, I_{ql} stand for the $d-$ and $q-$ axis output currents of the grid side voltage source converter, while m_d and m_q represent the $d-$ and $q-$ axis duty-ratio components of the converter, respectively. In addition, V_d, V_q stand for the $d-$ and $q-$ axis components of the voltage across the filter capacitance. Finally, ω_{grid} relates to the synchronous angular frequency of the filter that equals to the nominal angular frequency of the grid ω_n, while ω_{pll} represents the frequency produced by the PLL synchronism circuit, as described in section III. Also, $I_{load,ac,d}$, $I_{load,ac,q}$, $I_{res,ac,d}$, $I_{res,ac,q}$ stand for the $-d$ and $q-$axis components of the considered load and RES in the ac side, respectively, while $I_{gen,ac,d}$, $I_{gen,ac,q}$ stand for stand for the $-d$ and $q-$axis components of the considered generators injection in the ac side. All other parameters and their values are provided in the Table II.

D. Power Electronics converters

Concerning the adopted power electronic converter, a dc/dc bidirectional boost converter for energy storage component and a bidirectional ac/dc voltage source converter that enables a continuous power exchange capability, are embraced. In both cases, the average models of the converters are adopted with

states and inputs in the synchronously rotating $d-q$ reference frame, [14], [21] to be considered as in eq. (15)-(17).

$$L_{sc} \cdot \dot{I}_{sc} = -R_s \cdot I_{sc} - V_{c1} - m_{sc} \cdot V_{dc} + V_o \quad (15)$$

$$L_{bat} \cdot \dot{I}_{bat} = -R_{ser} \cdot I_{bat} - V_s - V_l - m_{bat} \cdot V_{dc} + V_o \quad (16)$$

$$C \cdot \dot{V}_{dc} = m_{bat} \cdot I_{bat} + m_{sc} \cdot I_{sc} - \frac{V_{dc}}{R_{dc}} - \\ - \frac{3}{4} \cdot (m_d \cdot I_{dl} + m_q \cdot I_{ql}) + I_{res,dc} - I_{load,dc} + I_{gen,dc} \quad (17)$$

where V_{dc} represents the dc-link voltage and R_{dc} stands for the resistance of the dc load connected to the dc-link. In addition, $I_{load,dc}$, $I_{res,dc}$, and $I_{gen,dc}$ stand for the considered load, RES, and generators injections in the dc side of the system, respectively. All related parameters are provided in Table II.

TABLE II: Parameters' values

Component	Parameter	Description	Value
Battery	R_{ser}	Series output resistance	0.0745 Ω
	R_S	Short term resistance	0.0467 Ω
	C_S	Short term capacitance	703.6 F
	R_L	Long term resistance	0.0498 Ω
	C_L	Long term capacitance	4475 F
	L_{bat}	Inductance of the boost converter	100 mH
	C_{cap}	Capacitance of the Battery	3060 F
Supercapacitor	R_{sc}	Series resistance	0.2 mΩ
	C_{sc}	Series capacitance	4365 F
	R_{c1}	Parallel branch resistance	0.0547 mΩ
	C_1	Parallel branch capacitance	2182 F
	L_{sc}	Inductance of the boost converter	50 mH
PCC	C	Capacitance at the PCC	1540 μF
	R_{dc}	dc auxiliary load	1000 Ω
LCL filter	L_f	Inverter-side inductance	0.48 mH
	L_g	Grid-side inductance	0.69 mH
	C_{fg}	Filter Capacitor	165 μF
	r_f	Inverter-side resistance	0.4 Ω
	r_g	Grid-side resistance	0.7 Ω
	R_{fg}	Damping resistance	3000 Ω
Grid	$V_{d,grid}$	d-axis grid voltage component	0
	$V_{q,grid}$	q-axis grid voltage component	20 kV

III. PROPOSED CONTROL SCHEME

The design and implementation of suitable control schemes that ensure an optimal system operation despite the grid disturbances that may occur has a great importance. The

proposed distributed control acts locally on the power electronic interfaces in an efficient and stable manner aiming to regulate the frequency and dc and ac voltages, during the transients occurring when the flexibility is activated real-time. The most considerable control goals include the operation of the HESS under constant voltage and grid's stable operation under constant voltage and frequency. To satisfy the aforementioned control goals, cascaded PI controllers are proposed and implemented. Fast inner-loop current controllers are used to compensate via the current variable the disturbance action very quickly, while the outer-loop controller eliminates the difference between the controlled current variable and its reference signal [16], [17].

A. Inner-loop current controllers

In particular, four cascaded PI feedback controllers are designed and implemented, one for each duty-ratio input signal. The general form of the proposed inner-loop controllers is provided by eq. (18). All inner-loop current controllers regulate the I_{dl}, I_{ql}, I_{bat}, and I_{sc} to each reference value, respectively, as provided by the outer-loop controllers and based on the desired design operation conditions.

$$m_i = \frac{1}{V_{dc}} \cdot [k_{P,i} \cdot (I_i - I_i^{ref}) + k_{I,i} \cdot \int_0^t (I_i - I_i^{ref}) \cdot d\tau]$$
(18)

where i stands for $dl-$, $ql-$, $bat-$, $sc-$ (representing the four control inputs), $k_{P,i}$ and $k_{I,i}$ are positive constants and stand for the controllers' gains, while I_i^{ref} represents each current reference value.

B. PLL and frequency control

The outer-loop controllers that provide the reference values to the inner ones are chosen as simple PI controllers. In particular, a PLL is designed and implemented within the I_{dl}^{ref} signal, eq. (19), that actually regulates the system frequency as close to the grid frequency ω_{grid} as possible. The latter is achieved via the $d-$axis grid voltage component V_d regulation to zero, eq. (20). After the synchronization of the PLL frequency with the one of the grid, the voltage source converter $d-$axis current component I_{dl}^{ref} tends to become zero, a fact that ensures unity power factor operation and consequently zero reactive power injection to the grid. The related to I_{ql}^{ref} reference signal controller, eq. (21), aims at regulating the $q-$axis grid voltage component to its desired constant value $V_q^{ref} = 20\,kV$. This control structure is related with ac voltage and frequency services provision (see section IV).

$$I_{dl}^{ref} = k_{P,d} \cdot (\omega_{pll} - \omega^{ref}) + k_{I,d} \cdot \int_0^t (\omega_{pll} - \omega^{ref}) \cdot d\tau$$
(19)

$$\omega_{pll} = \omega_n - k_{P,pll} \cdot V_d - k_{I,pll} \cdot \int_0^t V_d \cdot d\tau$$
(20)

$$I_{ql}^{ref} = -k_{P,q} \cdot (V_q - V_q^{ref}) - k_{I,q} \cdot \int_0^t (V_q - V_q^{ref}) \cdot d\tau$$
(21)

where $k_{P,d}, k_{I,d}, k_{P,pll}, k_{I,pll}, k_{P,q}$, and $k_{I,q}$ stand for the described controller gains and are positive constants.

C. HESS and dc voltage control

The outer-loop controllers related to HESS are constructed accordingly. A PI-controller is proposed for each storage system duty-ratio input and regulates the dc-link voltage to a predefined constant reference value V_{dc}^{ref} selected to support the converters duty-ratio operation under SPWM, eq. (22) and (23). In terms of flexibility services the main task of these controllers is related to peak shaving services (see section IV).

$$I_{bat}^{ref} = -k_{P,bat} \cdot (V_{dc} - V_{dc}^{ref}) - k_{I,bat} \cdot \int_0^t (V_{dc} - V_{dc}^{ref}) \cdot d\tau$$
(22)

$$I_{sc}^{ref} = -k_{P,sc} \cdot (V_{dc} - V_{dc}^{ref}) - k_{I,sc} \cdot \int_0^t (V_{dc} - V_{dc}^{ref}) \cdot d\tau$$
(23)

where $k_{P,bat}, k_{I,bat}, k_{P,sc}, k_{I,sc}$ stand for the controller gains and are positive constants.

Here it should be noticed that all controllers' gains are extracted via a systematic procedure as described in detail in [22].

IV. CASE STUDY - SIMULATION RESULTS

The complete HESS to grid system with the proposed cascaded controllers were implemented and examined through extended simulations on a Matlab/Simulink environment. All components and system parts have been accurately implemented by their mathematical models and the relevant parameters are provided in section II. The considered load in both ac and dc sides (used for $I_{load,ac,d}$, $I_{load,ac,q}$, $I_{load,dc}$, calculation) follows the arbitrarily down scaled waveform of the total real system load consumed within the Greek transmission system, [23], in a two day period, given in **Fig. 2**. In a similar manner, the considered RES generation follows a down scaled pattern of the real RES injection. The latter is in all cases smaller than the load and authors choose not to provide the waveform due to limited space reasons and its not critical nature for the results comprehension. Also, in all simulated attempts we assume that the rest load is provided by generators dispatched within the day ahead and intraday markets. Therefore, our control system is oriented to real-time imbalances that mainly occur during balancing energy market and specifically during delivery time. The obtained closed-loop system, after the proposed controllers integration, is examined for its robust operation in three different scenarios linked to ancillary services provision to the grid in real-time, as described below.

A. Peak shaving service

The first scenario involves the provision of peak shaving services to the grid, a process that lowers and smooths out the peak load. **Fig. 3** illustrates the power exchange between the system parts, i.e the battery, the SC, the entire HESS and the grid. It is clearly seen that the HESS (red line) provides

the excessive power in case of peak load (green line). In addition, based on the proposed power shaving technique the SC undertakes the power within the peak transient, while the battery provides the small amount of the demanded average power (black line). The latter observation is reinforced by the resulting SoC of the two sources, presented in **Fig. 4**. The battery's SoC slightly changes during the peak shaving provision, since the SC injects the most of the demanded power as shown by its SoC.
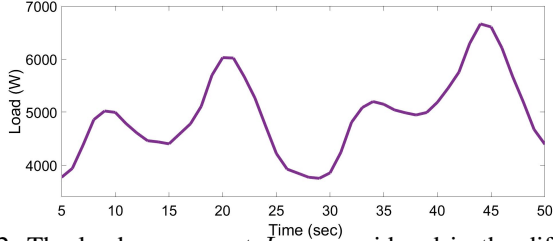

Fig. 2: The load component I_{load} considered in the different scenarios.
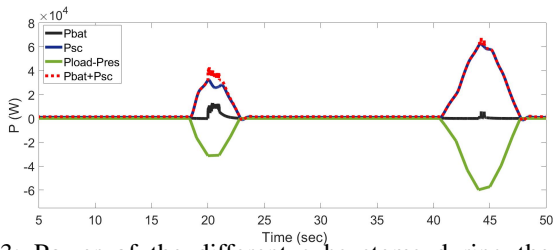
Fig. 3: Power of the different subsystems during the peak shaving service.
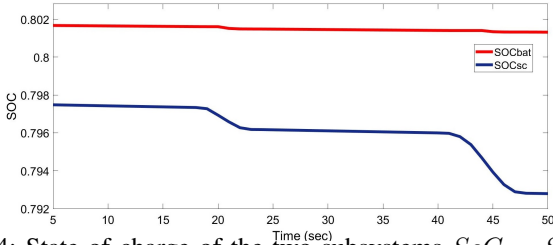
Fig. 4: State of charge of the two subsystems SoC_{bat}, SoC_{sc} of the HESS during peak shaving service.

B. Voltage control service

In the second scenario, the voltage control service is examined. In particular, a piece-wise constant change in the $q-$axis component of the grid voltage $V_{q,grid}$ is presented in the **Fig 5**. As it can be observed, the power exchange between the system components ensures the robust operation of the HESS during a voltage control service provision.

The resulting $q-$axis voltage component in the converter side, **Fig. 6**, is almost constant at the $V_{q,grid}$ reference value and slightly changes during the transients (service provision). The demanded power is provided/ absorbed from /to the grid by the SC source while the battery is almost idle, **Fig. 7**. The latter is also easily concluded from the resulting SoC curve of the battery that remains constant compared to the SC's one that varies, as depicted in **Fig. 8**.
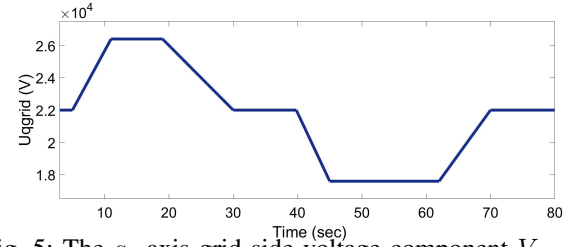

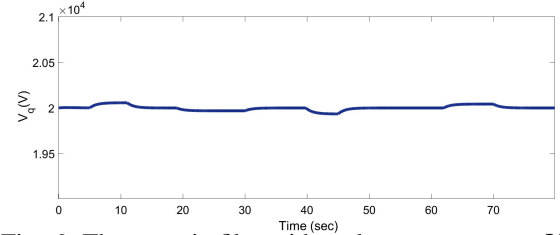Fig. 5: The $q-$axis grid side voltage component $V_{q,grid}$.

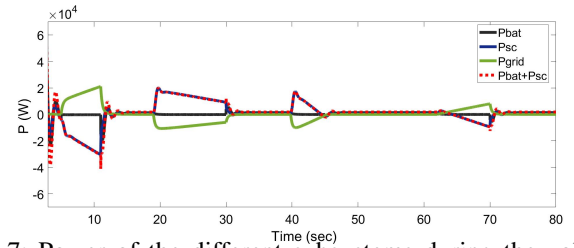Fig. 6: The $q-$axis filter side voltage component V_q.

Fig. 7: Power of the different subsystems during the voltage control service.
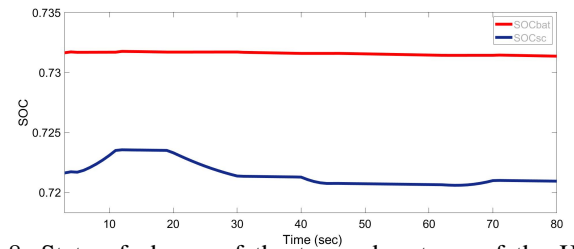

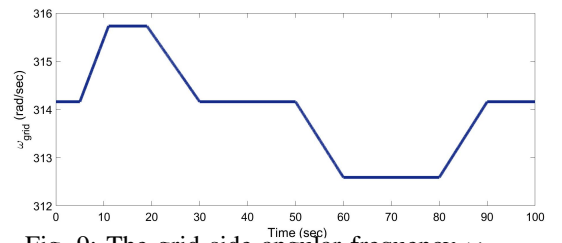Fig. 8: State of charge of the two subsystems of the HESS SoC_{bat}, SoC_{sc} during voltage control service.

Fig. 9: The grid side angular frequency ω_{grid}.

C. Frequency control service

Lastly, the third scenario is related to frequency control service. More specifically, a piece-wise constant change in the grid's frequency is portrayed in the **Fig. 9**.

Figure 10 indicates that the proposed control scheme regulates the ω_{pll} angular frequency close to the nominal grid angular frequency ω_n. The power curves of all the system's

components, **Fig. 11**, indicate a stable and proper operation of the HESS system, when provides frequency service to the grid since it completely supplies the demanded power. Again, the battery provides the majority of the demanded energy, while the SC undertakes the power provision during transients. The latter is also depicted in the SoC waveforms of the two sources, **Fig. 12**.
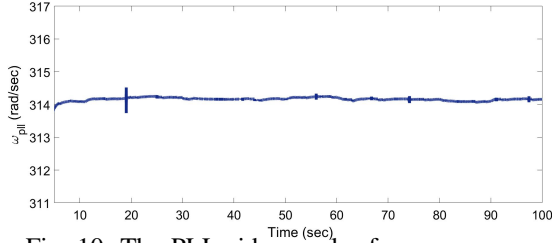

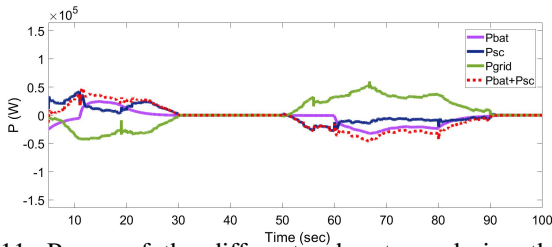Fig. 10: The PLL side angular frequency ω_{pll}.

Fig. 11: Power of the different subsystems during the frequency control service.
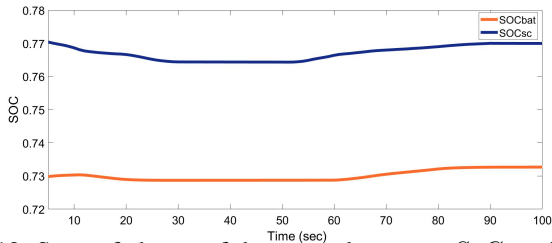

Fig. 12: State of charge of the two subsystems SoC_{bat}, SoC_{sc} of the HESS during frequency control service.

V. Conclusions

In this paper, the need for flexibility within the power system to compensate for variability in supply and demand and maintain its balance, is investigated. The problem arises due to the inherent intermittent and stochastic nature of RES which is constantly modifying the time dynamics of the modern power grids, increasing the unpredictability. The solution proposed here, includes a HESS, a combination of battery and SC. Regarding the literature, the hybridization of the storage systems is a recent trend. A HESS can tackle the frequency and voltage transients; however, an advanced control strategy is required. Power electronic devices offer a critical opportunity for controlling the power transferred through them. In this manner, flexibility needs can be met in a real-time level guaranteeing the balancing between RES production, load and grid fluctuations. Control structures based on hierarchical schemes and PI forms are applied for the overall system that examined, while for convenience reasons the system modeling and controllers' deployment are designed at the synchronously rotating $d - q$ reference frame. The

HESS is evaluated under extended simulations, under varying conditions, offering flexibility services locally to the grid. The results extracted verify the control schemes' robustness, the quick and smooth system's response.

References

[1] W. Yi, D. J. Hill and Y. Song, "Impact of High Penetration of Renewable Resources on Power System Transient Stability, *IEEE Power & Energy Society General Meeting (PESGM)*, Atlanta, GA, USA, 2019, pp. 1-5.

[2] B. Mohandes, M. S. E. Moursi, N. Hatziargyriou and S. E. Khatib, "A Review of Power System Flexibility With High Penetration of Renewables," *IEEE Transactions on Power Systems*, vol. 34, no. 4, pp. 3140-3155, July 2019.

[3] O.M. Babatunde, J.L. Munda, and Y. Hamam, "Power system flexibility: A review", *Energy Reports*, vol. 6, no. 2, pp. 101-106, 2020.

[4] Lawrence E. Jones (ed.), *Renewable Energy Integration*, 2nd ed., Academic Press, pp. 309-316, 2017.

[5] D. Koolen, M. De Felice, and S. Busch, "Flexibility requirements and the role of storage in future European power systems", *Publications Office of the European Union*, Luxembourg, 2023.

[6] G. Pistoia (editor), *Lithium-Ion Batteries: Advances and Applications*, Elsevier, 2014.

[7] V. Musolino, E. Tironi and P. di Milano, "A comparison of supercapacitor and high-power lithium batteries," Electrical Systems for Aircraft, Railway and Ship Propulsion, Bologna, Italy, pp. 1-6, 2010.

[8] U. Manandhar, A. Ukil , H.B Gooi, N.R Tummuru, S.K Kollimalla, B. Wang and K. Chaudhari, "Energy Management and control for grid connected hybrid energy storage system under different operating modes", IEEE Trans. Smart Grid, vol. 10, pp 1626-1636, 2019.

[9] T. Barath, M. Ragupathi, E. Anand Issack, G.V.S Pavankummar, "Supercapacitor Based Power Conditioning System for Power Quality Improvement in Industries", IJERT, vol. 4, 2015.

[10] T.A Nguyen, V.T Nguyen, K. Hur, J.W Shim, " Coordinated Control of a Hybrid Energy Storage System for Improving the Capability of Frequency Regulation and State-of-Charge Management", Energies, vol. 13, 2020.

[11] J. Arkahangelski, P. Roncero-Sanchez, M. Abdou-Tnakari, J. Vasquez, G. Lefebvre, " Control and restrictions of a hybrid renewable energy system connected to the grid: A battery and supercapacitor storage case ", Energies, vol. 12, 2019.

[12] J. Rocabert, R. Capo-Misut, R.S Munoz - Aguilar, J.I Candela, P. Rodriguez, " Control of Energy Storage System Integrating Electrochemical Batteries ans Supercapacitors for Grid-Connected Applications", IEEE Trans. Ind. Appl., vol. 55 pp 1853-1862, 2019.

[13] A.M.A Malkawi, L.A.C Lopes, "Improved dynamic voltage regulation in a droop controlled DC nanogrid employing independently controlled battery and supercapacitor units ", Appl. Sci. vol. 8, 2018.

[14] A. Yasdani, R. Iravani, *Voltage-sourced converters*, Hoboken NJ:IEEE/Wiley, 2010.

[15] D. I. Makrygiorgou, A. T. Alexandridis, "Distributed stabilizing modular control for stand-alone microgrids", *Applied Energy*, vol. 210, pp. 925-935, 2018.

[16] F. Haugen, *Basic Dynamics and Control*, TechTeach: Skien, Norway, 2010.

[17] K.J. Astrom, R.M. Murray, *Feedback Systems - An Introduction for Scientists and Engineers*, Princeton University Press: Princeton, NJ, USA, 2008.

[18] M. Chen and G.A. Rincon-Mora, "Accurate electrical battery model capable of predicting runtime and I-V performance," *IEEE Trans. on Energy Conversion*, vol. 21, no. 2, pp. 504-511, June 2006.

[19] R. de Levie, "On porous electrodes in electrolyte solutions," *Electrochimica Acta*, vol. 8, no. 10, pp. 751 – 780, 1963.

[20] A. Reznik, M. G. Simoes, et. al., "LCL Filter Design and Performance Analysis for Grid-Interconnected Systems," *IEEE Trans. on Industry Applications*, vol. 50, no. 2, pp. 1225-1232, 2014.

[21] N. Mohan, T. M. Underland, and W. P. Robbins, *Power electronics*, 3rd edn, John Wiley, 2003.

[22] J.J. Makrygiorgou, and A.T. Alexandridis, "Unified Modeling, Control and Stability for a Vehicle to grid and Plug-in EV System," *IEEE Journal of Emerging and Selected Topics in Power Electronics*, 2020.

[23] IPTO. Market statistics - Data. (2021) Available online: https://www.admie.gr/en/market/market-statistics/detail-data